NASA TECHNICAL NOTE

NASA TN D-4201

NASA TN D-4201

INVESTIGATION OF THE DYNAMICS OF WATER REJECTION FROM A HYDROGEN-OXYGEN FUEL CELL TO A HYDROGEN STREAM

by Paul R. Prokopius and Norman H. Hagedorn

Lewis Research Center
Cleveland, Ohio

NATIONAL AERONAUTICS AND SPACE ADMINISTRATION • WASHINGTON, D. C. • OCTOBER 1967

NASA TN D-4201

INVESTIGATION OF THE DYNAMICS OF WATER REJECTION FROM A HYDROGEN-OXYGEN FUEL CELL TO A HYDROGEN STREAM

By Paul R. Prokopius and Norman H. Hagedorn

Lewis Research Center
Cleveland, Ohio

NATIONAL AERONAUTICS AND SPACE ADMINISTRATION

For sale by the Clearinghouse for Federal Scientific and Technical Information
Springfield, Virginia 22151 – CFSTI price $3.00

INVESTIGATION OF THE DYNAMICS OF WATER REJECTION FROM A HYDROGEN-OXYGEN FUEL CELL TO A HYDROGEN STREAM

by Paul R. Prokopius and Norman H. Hagedorn

Lewis Research Center

SUMMARY

A water-rejection-dynamics study of a hydrogen-oxygen fuel cell was conducted using both experimental and analytical techniques. In the type of cell studied, water resulting from the fuel-cell reaction diffuses as a vapor through a porous electrode and is removed by circulating gaseous hydrogen.

The experimental investigation was conducted by introducing step transients in the rate of water production and in the inlet humidity of the water-removal gas stream, while holding all other cell operating parameters constant. The resulting water-rejection transients were measured as changes in outlet-stream humidity. These transients were very slow, taking 1 hour or longer to reestablish a steady-state operating condition in which the water being removed by the hydrogen stream just equals that formed by the cell reaction. Step transients were also introduced with the electrolyte at an initial "dried-out" condition, which caused a slowing down of the rejection response.

In the analytical portion of the study, a mathematical model of the water-rejection mechanism was derived. The resulting model is in the form of a linear, first-order differential equation. When the various dimensions and operating conditions of the cell tested were substituted for the corresponding constants of the mathematical model, its step response was calculated and was found to compare well with the experimental data.

INTRODUCTION

Hydrogen-oxygen fuel-cell systems occupy an important position among power supplies for manned space missions such as Gemini, Apollo, and the Manned Orbiting Laboratory (MOL). The power profiles of missions such as these can vary from the minimum design level to emergency overloads 50 percent above the design output. During and after

changes in power level, safe and efficient operation should be maintained by a control system associated with the fuel cells. One function of the control system is to keep the electrolyte concentration of the cells within acceptable limits by regulating the rate of rejection of the water formed by the electrochemical reaction.

One technique of removing water from a hydrogen-oxygen fuel cell is to circulate through the cell an amount of hydrogen in excess of that consumed in the electrochemical reaction. In this technique, the water produced by the reaction is transported by vapor diffusion through the porous electrode and into the circulating gas stream. Thus, regulating the flow rate and the humidity of the circulating hydrogen stream controls the rate of water rejection and, thereby, maintains the desired value of electrolyte concentration. Among the factors requiring consideration in designing the system that produces this conditioned circulating gas stream are the responses of the cell water-rejection rate to changes in the rate of water production (cell power) and to changes in the circulating-stream inlet humidity.

Therefore, a study was conducted of the water-rejection dynamics of a hydrogen-oxygen fuel cell. This study was conducted to gain a better understanding of the water-rejection processes of some of the cells presently in use, with the belief that the knowledge gained would aid in the design of water-removal controls of future fuel-cell systems. Both experimental and analytical methods were used in the study.

The experimental portion of the program utilized a module consisting of Bacon-type cells similar to those to be used on the Apollo mission. These cells, which operate near 400° F (204.4° C), use a molten electrolyte which is contained between dual-porosity electrodes. The electrolyte, a solution of potassium hydroxide (KOH) in water, contains approximately 75-percent KOH. A hydrogen-control-stream simulator was developed to introduce transients in the humidity of the hydrogen stream entering the fuel cells, while maintaining constant stream pressure, temperature, and flow rate. Module output-power transients were introduced by increasing the module load-resistance setting. For both the power and inlet-humidity transients, the resulting dynamics in the water-rejection process were determined by measuring the humidity response of the hydrogen stream at the module outlet. These humidity changes were monitored by a continuous-reading humidity sensor, the basis of which is a fluidic oscillator (ref. 1).

In the analytical portion of the study, a mathematical model was constructed which considered the water rejection from an isothermal, two-dimensional, hydrogen-oxygen fuel cell. The analysis was based on the conservation of mass in the electrolyte and the diffusion of water vapor through the hydrogen - water-vapor mixture in the porous hydrogen electrode. The resulting equation was evaluated in terms of the dimensions and physical properties of one of the fuel cells of the module, which was studied experimentally. When the various conditions at which the cell was operated during the experimental transients were used, the response of the model was calculated and compared with the corresponding experimental response.

APPARATUS AND INSTRUMENTATION

Fuel Cell

A schematic diagram of a Bacon-type fuel cell, of the type used in the module tested, is shown in figure 1. In this high-temperature cell an electrolyte consisting of a concentrated mixture of potassium hydroxide and water is contained between dual-porosity, sintered nickel electrodes which are mounted with the fine-pore structure toward the electrolyte. The hydrogen and oxygen reactants are supplied to the cell through gas chambers adjacent to the electrodes. The electrolyte, which for this cell is at atmospheric pressure, is contained within the electrodes by maintaining a positive pressure in the reactant chambers. This pressure is great enough to overcome the capillary forces of the electrolyte in the coarse pores of the electrode but is not great enough to overcome those forces in the fine pores. The result is that the electrolyte is held within the fine-pore structure.

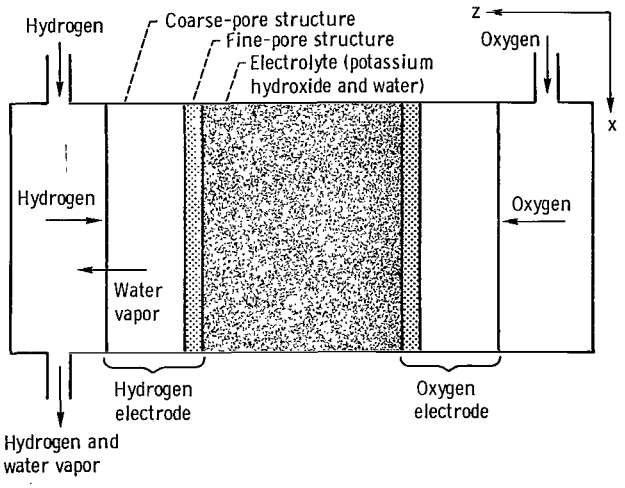

Figure 1. - Schematic of fuel cell used in tests.

Heat and water, the reaction byproducts, are removed from the cell by flowing a controlled excess of hydrogen through the hydrogen gas chamber. The amount of heat removed by the hydrogen stream is controlled by the stream temperature at the cell inlet. The water, in vapor form, diffuses through the hydrogen electrode to the hydrogen supply chamber, where it is removed from the cell by the hydrogen stream.

The module tested was constructed of 15 cells electrically connected in series to give a design power level of 250 watts at approximately 15 volts. It was operated in an oven, and electric heaters were built into the module to attain the temperature necessary for startup and to help maintain the module operating temperature at low power levels.

Test Apparatus

The hydrogen-reactant supply apparatus was designed with the capability of supplying the fuel-cell module with a hydrogen-steam mixture at controlled temperature, pressure, flow rate, and humidity. The remotely controlled test apparatus with the fuel-cell module (oven hood removed) in position is shown in figure 2. In addition to automatically main-

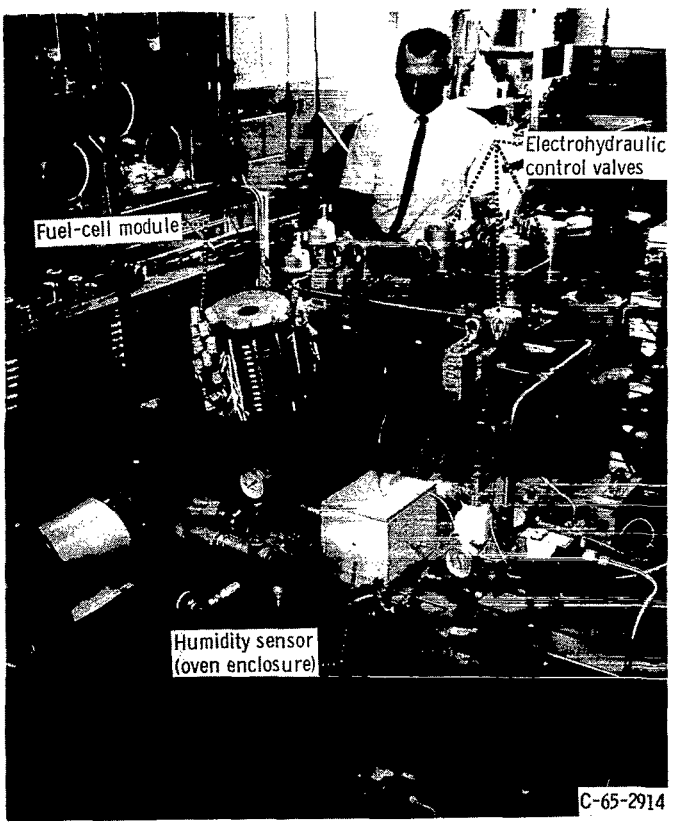

Figure 2. - Test apparatus and fuel-cell module.

taining the desired set points of the various hydrogen-stream control parameters, the apparatus was designed with the capability to produce controlled perturbations in any one of the parameters while holding all others at the initial set-point values. This characteristic of individual parameter control provided the ability to isolate the effects that any one input transient had on the fuel cell. The characteristics emphasized in the design of the test apparatus were parameter-control accuracy and the speed at which a stream transient could be produced. Consequently, the water-vapor and hydrogen flow rates and stream pressure were controlled to within 0.1 percent of the set points, and the stream temperature was controlled to within 1^{o} of a fixed setting. Flow-rate, stream-pressure, and humidity transient ramps with magnitudes of 20 percent of the steady-state set points can be produced in approximately 15 seconds, while a 20-percent ramp in stream temperature takes approximately 30 seconds.

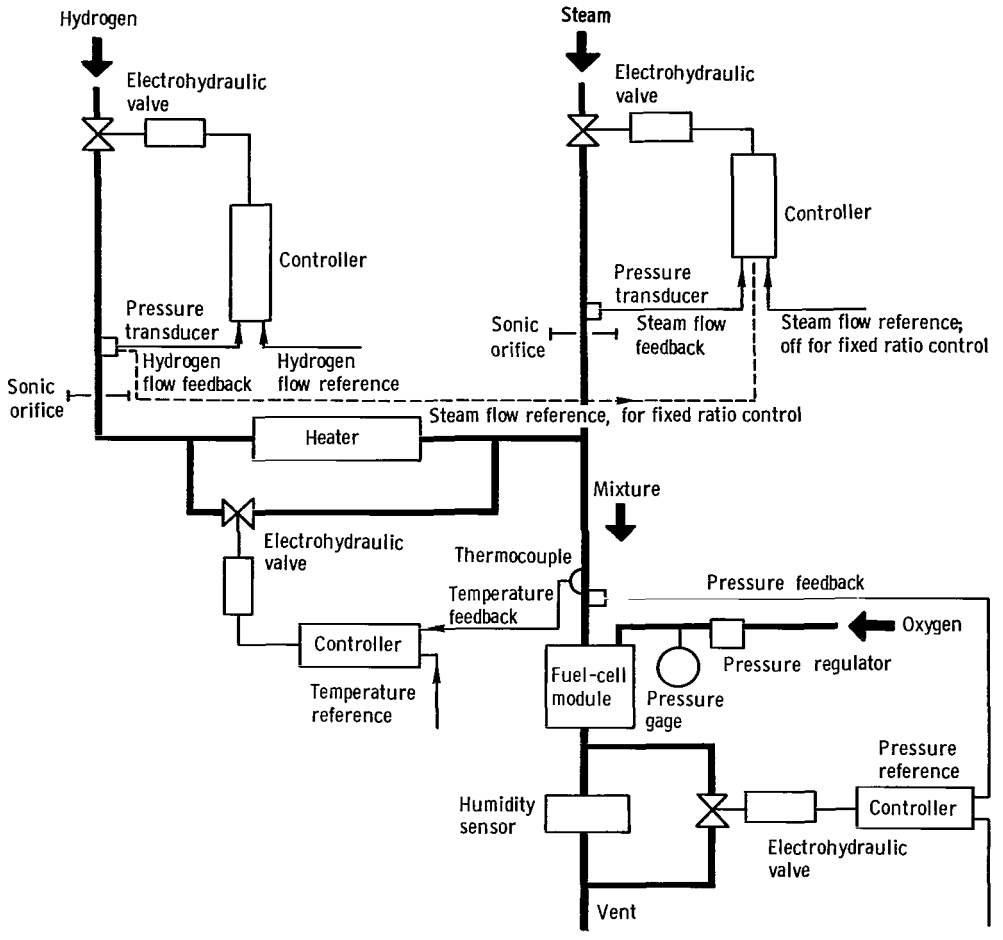

Figure 3. - Schematic diagram of fuel-cell dynamics test apparatus.

As shown in the schematic diagram (fig. 3), the test apparatus was composed of four closed-loop control systems. A humidified hydrogen stream was produced by mixing superheated steam with heated hydrogen. The flow rate of each component in the hydrogen - water-vapor mixture was set by controlling the pressure upstream of a sonic flow orifice in each line. Using individual hydrogen and steam flow control gave the capability to maintain conditions or to introduce transients into the mixture ratio (humidity). The introduction of transients in the total flow rate of the mixture, while maintaining a constant mixture ratio, would require the slight change in controller configuration shown by the dashed lines in figure 3.

Temperature control of the humidified stream at the inlet of the fuel cell is achieved by controlling the temperature of the hydrogen portion of the stream. This control is accomplished by using the cell-inlet mixture temperature as the feedback signal for a hydrogen temperature-control loop. Proportioning room-temperature hydrogen gas through or around a manually controlled, fast-response heater allowed variation of the hydrogen gas temperature, which, in turn, provided the desired mixture temperature.

Control of the humid-hydrogen-stream pressure at the fuel-cell inlet was attained by controlling the position of a vent-line valve located downstream of the test component. Control of the oxygen gas chamber pressure was provided by a manually operated pressure regulator, which was installed in the oxygen supply lines. This component was the only one required since the oxygen side of the fuel cell was dead-ended.

Integral-proportional control was used in the various system-control loops. This control was achieved by building up the controller circuits on a transistorized analog computer, which was installed in the control room. The computer was used because it provided a concentration of highly accurate, flexible, drift-free electronic equipment, which lends itself very well for use in controller circuitry.

Instrumentation

The recording equipment that was used included the following components:

(1) A digital voltmeter to check pertinent module and test-apparatus parameters during operation

(2) Strip chart recorders to record stream-input and transient data, selected module temperature, and cell-power data

(3) A profile monitor to provide a visual display of 15 cell and 20 test-rig temperatures which were, in turn, used as references in making module and test-apparatus heater settings

The fuel-cell module was instrumented with thermocouples, which were installed between each cell and at various points in the inlet and outlet stream. Pressure instrumentation internal to the module was unnecessary since, for the operating flow rates, experience has shown that a negligible pressure drop exists through the cell gas chambers and supply manifolds. Thus, the control pressure upstream of the module was assumed to be the hydrogen-stream pressure throughout the cell.

The various test-apparatus control-loop feedback pressures were measured with high-temperature, fast-responding (natural frequency, 6000 cps) strain-gage pressure transducers, which were mounted with a minimum of tubing volume from the flow stream to the diaphragm.

Thermocouples were installed on the electrohydraulic control valves and at regular intervals along the length of the rig tubing to obtain a temperature profile of the heated test apparatus. A thermocouple was inserted into the flow stream upstream of the steam sonic orifice. This temperature served as a reference by which to manually set the steam superheater temperature and, thereby, to maintain the steam at the temperature for which the orifice was calibrated. A fast-response, open-ball thermocouple was installed at the fuel-cell inlet to provide the reference for the mixture temperature-control loop.

The instrument used to measure the humidity (steam to hydrogen mass ratio) of the fuel-cell-outlet hydrogen stream was a continuous-reading inline device. The basis of the instrument is a fluidic oscillator with a frequency of oscillation sensitive to the molecular weight or mass ratio of the stream in question. The instrument displayed good accuracy (±2 percent) and a frequency response which was flat at least to 3 cycles per second (ref. 1).

TEST PROCEDURE

With the module reactant chambers purged with nitrogen, the intercell and module oven heaters were used to bring the module up to operating temperature (400° F (204.4° C)). Once operating temperature was attained, the reactants were introduced and the load was applied. For a given operating power level, the hydrogen stream was circulated through the module at the recommended flow rate (viz, one which maintains the electrolyte within the design concentration range of the cells). A steady-state operating condition was achieved when the startup transients in the continuously monitored parameters of cell temperature, voltage, current, and outlet stream humidity were completely damped out.

Once steady state was attained, dynamics tests were conducted by disturbing the inlet hydrogen humidity or the output power of the module and by recording the response of the outlet hydrogen humidity. The inlet hydrogen disturbances were ramp functions; however, since the speed of the input ramps was extremely fast compared with the speed of the resulting transients, the data could be assumed to be that of step response. The input stream temperature and pressure were automatically held constant during these inlet humidity transients. The magnitudes of the humidity changes that were introduced ranged from 15 to 50 percent. For changes in the rate of water formation, stream parameters were automatically held constant and increases (up to 100 W in magnitude) were introduced into the cell output power (current) by load resistor switching.

A similar procedure was followed in running the transients with the electrolyte at a dried-out initial condition, except that during pretransient operation a flow of hydrogen higher than that recommended for the particular operating power level was circulated through the cells. This increased hydrogen flow reduced the net amount of water in the electrolyte and, thereby, produced the desired dried-out (concentrated) initial electrolyte concentration.

During testing, the cells were made to eject a constant-temperature hydrogen stream. This ejection was accomplished by operating the module below its 250-watt rating (100 to 200 W). At lower than rated power conditions, the cells did not generate enough heat to be selfsustaining, and, therefore, by manually adjusting the intercell heaters, the cells were made to operate at a constant temperature.

EXPERIMENTAL RESULTS AND DISCUSSION

The response curves were normalized, to compare the results of the various transients directly, by plotting each data point as a percentage of the total change between the initial and final equilibrium values rather than as an actual value of stream mass ratio. The response data presented in table I and the corresponding response curves shown in

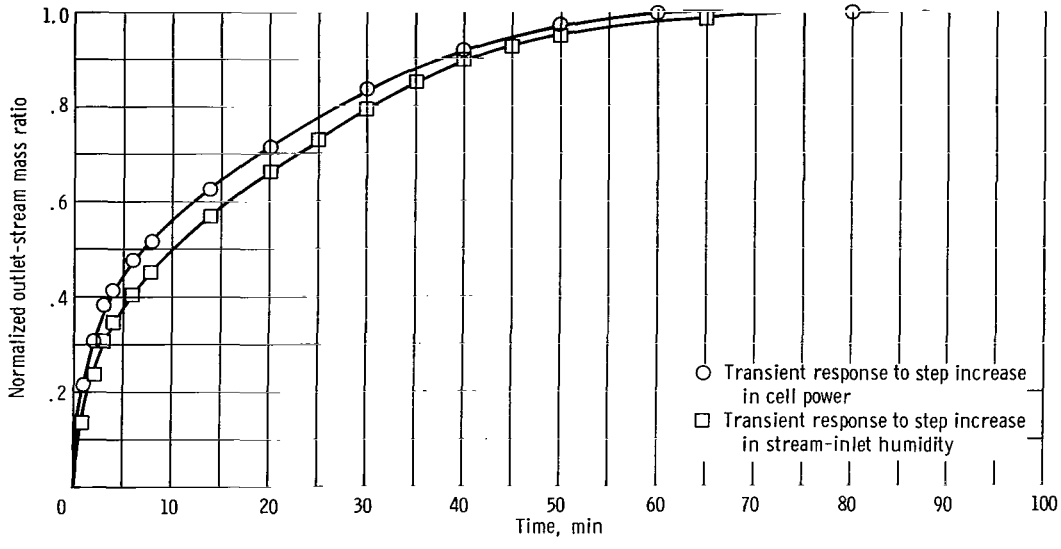

Figure 4. - Transient response of hydrogen-stream-outlet water vapor to hydrogen mass ratio with electrolyte concentration at design value.

figure 4 are for the case in which stream-input mass ratio and cell-power-level transients were introduced with the electrolyte concentration at design conditions. These curves, which are similar, approximate a first-order-lag response with a time constant of approximately 16 minutes. The similarity aspect and the fact that the response can be considered to be first order indicate that the same single capacitive effect provides the lag for both transients.

The stream mass-ratio and power-transient response curves of figure 4 are compared with the responses of similar transients introduced with the electrolyte in a dried-out condition in figures 5 and 6, respectively. Comparison of the curves plotted in figures 5 or 6 shows that a dried-out electrolyte retards the water-rejection response of the module; that is, a longer time is required to reestablish an equilibrium condition between the electrolyte concentration and the water-vapor to hydrogen mass ratio of the hydrogen stream.

For an extreme-condition test, the electrolyte was put in a very dry state by operating the module off a dry, high-flow-rate hydrogen stream for a considerable length of time. For an input transient, steam was injected into the hydrogen stream. The response to this transient, as shown in figure 7, differed from the data of figures 5 and 6 by

TABLE I. - MODULE OUTLET-STREAM MASS-RATIO (HUMIDITY)

DATA FOR TRANSIENTS AT DESIGN ELECTROLYTE CONDITIONS

Time, min	Recorded outlet mass ratio, $\left(W_{H_2O}/W_{H_2}\right)$	Normalized outlet mass ratio
Power step transient, 193.5 to 98.0 W		
0	1.033	-----
1	.933	0.218
2	.893	.305
3	.859	.380
4	.845	.410
6	.815	.475
8	.797	.515
14	.745	.628
20	.707	.712
30	.649	.837
40	.614	.915
50	.588	.970
60	.575	1.000
80	.575	1.000
Inlet mass-ratio step transient (inlet mass ratio, 0.745 to 1.20)		
0	1.660	0.000
1	1.662	.136
2	1.708	.238
3	1.738	.305
4	1.775	.344
6	1.782	.400
8	1.806	.453
14	1.858	.567
20	1.900	.660
25	1.929	.725
30	1.962	.796
35	1.986	.850
40	2.010	.901
45	2.021	.925
50	2.030	.945
65	2.045	.978
80	2.055	1.000
100	2.055	1.000

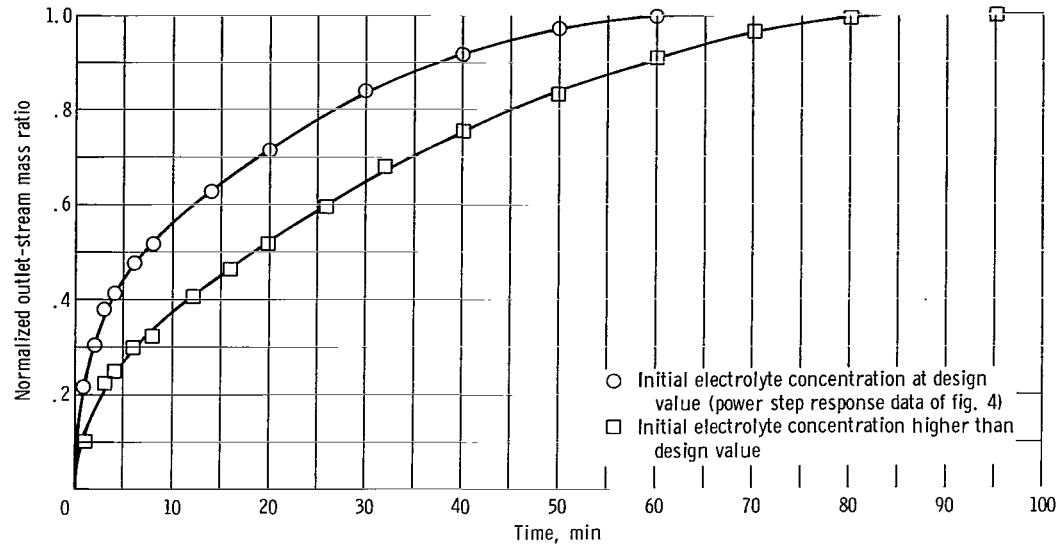

Figure 5. - Transient response of hydrogen-stream-outlet water vapor to hydrogen mass ratio to step increase in cell power.

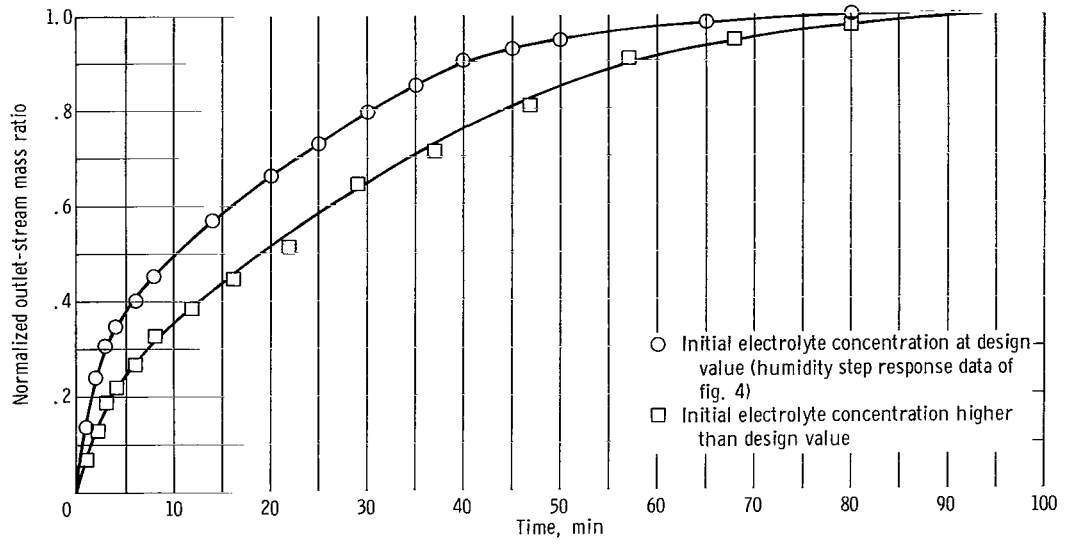

Figure 6. - Transient response of hydrogen-stream-outlet water vapor to hydrogen mass ratio to step increase in inlet-stream mass ratio.

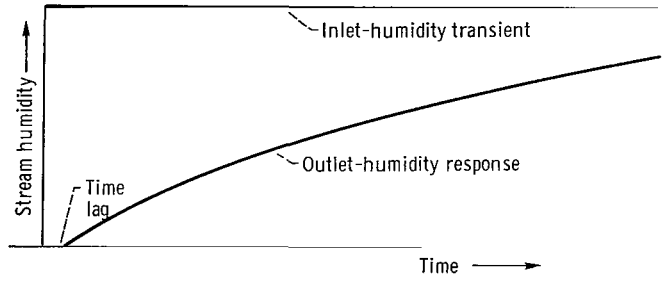

Figure 7. - Module outlet-humidity response to inlet-humidity step transient introduced with the electrolyte in an extremely dry state.

a small time delay in the outlet humidity, which occurred at the inception of the transient. This delay indicates that water was drawn from the hydrogen stream into the electrolyte. This effect was further evidenced by a fast 15° F (9.45° C) increase in cell temperature that was attributed to the heat of solution generated as a result of water absorption by the dry electrolyte.

THEORETICAL ANALYSIS

The theoretical analysis of the water-rejection dynamics is based on a lumped-parameter treatment of the conservation of the mass of water in the electrolyte. The resulting mathematical model, the derivation of which is presented in appendix A, is expressed as a linear, first-order differential equation. The dependent variable of the equation is the cell outlet-stream mass ratio H_o, and the independent variables are the inlet-stream mass ratio H_i and the water-production rate of the reaction W_r. The equation is

$$\frac{dH_o}{dt} + \frac{H_o}{\tau} = \frac{9W_r}{\varphi m_{KOH} P_{H_2,o}} + \frac{P_{H_2,i} H_i}{\tau P_{H_2,o}} \tag{A17}$$

where

$$\varphi = \frac{0.434\ B}{C^2 P_e}$$

and

$$\tau = \frac{Lm_{KOH}\varphi}{nA_z(\Delta Z_3)(1 - e^{-mL/n})}$$

where

$$n = \frac{9\overline{W}_{H_2}}{A_x \overline{P}_{H_2}}$$

and

$$m = \frac{0.89\, D_{H_2\text{-}H_2O}}{(\Delta Z_3)(\Delta Z_2)RT}$$

(Symbols are defined in appendix B.) The response of the outlet-stream mass ratio to a unit step in input-stream mass ratio or water-production rate can be calculated from equation (A17). The term τ is recognized as the time constant of the first-order lag response of the differential equation.

The derived mathematical model (eq. (A17)) predicts the conclusion drawn from the experimental data, which is that the concentration of the electrolyte affects the water-rejection response rate (time constant). This effect is evident in the expression for the time constant τ, which is inversely proportional to the product of the electrolyte vapor pressure and the square of the electrolyte concentration. The relation between this concentration and the vapor pressure is such that for an increase in concentration the product of the vapor pressure and the square of the concentration decreases. Thus, by putting the electrolyte in a dried-out (concentrated) state, this product is decreased, thereby increasing the time constant.

Operating data for the case in which transients were introduced with the electrolyte at design conditions, along with various test fuel-cell dimensions, are as follows:

Electrode coarse-pore thickness, ΔZ_2, in.; cm 0.070; 0.178

Gas-chamber thickness, ΔZ_3, in.; cm 0.04; 0.102

Gas-chamber length, L, in.; cm 22.0; 55.88

Gas-chamber, x-direction, cross-sectional area, $in.^2$; cm^2 . . . . . 0.0216; 0.1394

Average, steady-state, hydrogen flow rate through gas chamber, W_{H_2}, lb/sec; kg/sec . . . . . 0.463×10^{-5}; 0.210×10^{-5}

Average, steady-state, hydrogen partial pressure over length of gas chamber, $\overline{P}_{H_2}$, $lb/in.^2$; kg/cm^2 . . . . . 19.25; 1.353

Mass diffusivity of hydrogen - water-vapor mixture, $D_{H_2\text{-}H_2O}$, $in.^2/sec$; cm^2/sec 0.389; 2.509

Water-vapor gas constant, R, (in.-lb)/(lb mass)(^oR); (m-kg)/(kg)(^oK) 1030.0; 472.0

Cell operating temperature, T, ^oR; ^oK 860.0; 477.5

Proportionality constant relating electrolyte concentration and electrolyte partial pressure, φ, $in.^2/lb$; cm^2/kg 0.0257: 0.365

Mass of potassium hydroxide present in electrolyte, m_{KOH},
lb mass; kg 0.478:0.217

Electrode surface area, A_z, in.^{2}; cm^2 . . . . . 78.5:506.0

With this data the time constant τ was calculated to be 14.4 minutes. An exponential function with a time constant of 14.4 minutes $1 - e^{-t/14.4}$, which represents the response of the theoretical model, was plotted along with the comparable experimental response data in figure 8. A comparison of these data shows that the experimental and analytical responses are in good agreement.

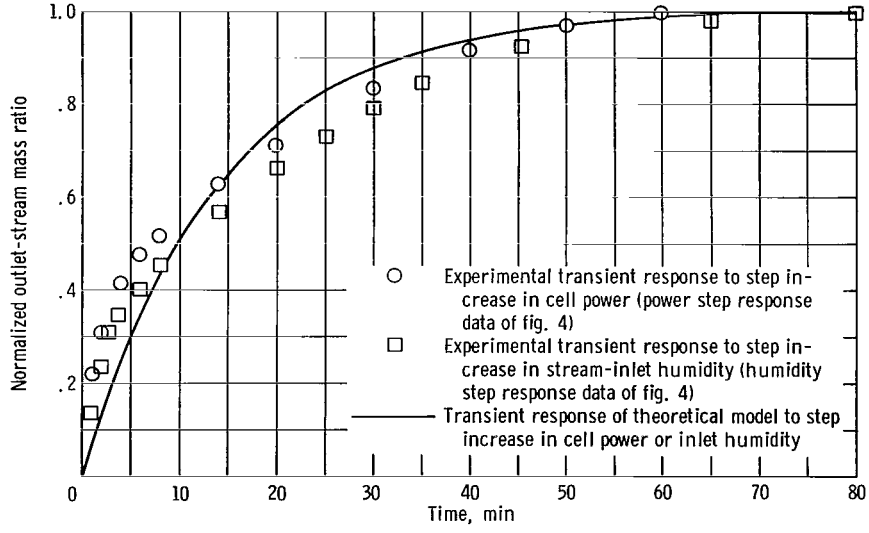

Figure 8. - Comparison of theoretical and experimental response for transients introduced with electrolyte initially at design concentration.

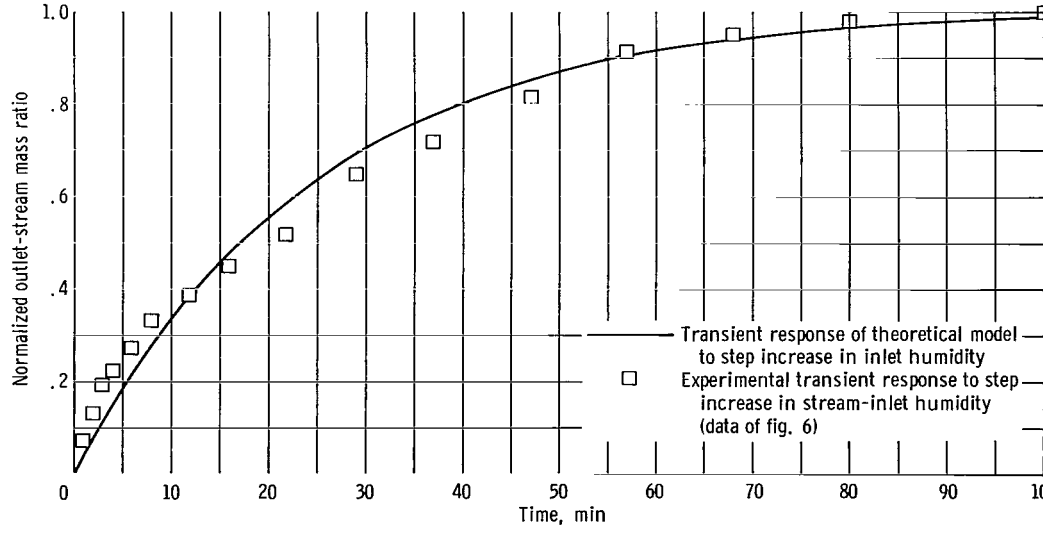

Figure 9. - Comparison of theoretical and experimental response for transient introduced with electrolyte at dried-out initial condition.

Experimental response data and the response of the mathematical model for the case in which an inlet-humidity transient was introduced with the electrolyte in a dried-out initial condition are shown in figure 9. For this case, the time constant τ was calculated to be 24.7 minutes, and again, the experimental and analytical response data agree well.

This agreement between the theoretical curves and the experimental data appears to validate the derived model. This validation indicates that the electrolyte water-storage capacity and electrode water-vapor diffusion are the governing factors in the water-rejection process and provides the basis for a simple mathematical description of the water-rejection mechanism of the fuel cell.

CONCLUSIONS

From the experimental water-rejection dynamics data and the theoretical analysis, the following conclusions can be drawn:

1. For step transients in inlet-stream humidity or cell power level, the experimental water-rejection response (outlet-stream humidity) approximated a first-order lag.

2. The electrolyte concentration, at the inception of a step transient in inlet-stream humidity or cell power, affected the time constant of the resulting water-rejection response. A dried-out electrolyte had the effect of slowing the response (increasing the length of the time constant).

3. A mathematical model was derived on the basis of the conservation of the mass of water in the electrolyte and vapor diffusion through the porous electrode. The response of the model to step transients in the inlet-stream humidity and the cell power agreed well with corresponding experimental response data. The agreement between the model and the data indicates that the capacitive effect of the electrolyte and the resistance to water-vapor diffusion through the electrode are the governing factors in the water-rejection dynamics. The effect of the electrolyte concentration on the transient-response time constants is also predicted by the mathematical model.

Lewis Research Center,
National Aeronautics and Space Administration,
Cleveland, Ohio,
120-34-02-01-22.

APPENDIX A

DERIVATION OF MATHEMATICAL MODEL

The mass-conservation equation for water in the electrolyte volume states that the rate of mass accumulation equals the rate of mass generation minus the rate of mass outflow. The equation can be written as

$$\frac{dm_{H_2O}}{dt} = W_r - W_e \tag{A1}$$

If the dynamic effects due to the electrode volume are assumed to be negligible, the water flow out of the electrolyte W_e is equal to the steady-state water-vapor flow in the hydrogen electrode and can be defined by applying Fick's first law of diffusion. This law is a steady-state equation that describes the movement of one component of a binary mixture caused by a concentration gradient of the component in question. On a molar flux basis, taking the outflow from the electrolyte to be along the z axis, the equation (ref. 2) is

$$N_{H_2O} = cD_{H_2\text{-}H_2O} \frac{dx_{H_2O}}{dz} + x_{H_2O}\left(N_{H_2O} + N_{H_2}\right) \tag{A2}$$

With the fuel cell operating in a steady-state condition, 1 mole of water vapor is rejected through the hydrogen electrode for each mole of hydrogen consumed by the reaction. Thus, the hydrogen electrode mass transfer is defined as being an equal-molar, counter-diffusion process. Since this is the case, the molar fluxes of water vapor and hydrogen are equal and in opposite direction, $\left(N_{H_2O} = -N_{H_2}\right)$, and Fick's law reduces to

$$N_{H_2O} = -cD_{H_2\text{-}H_2O} \frac{dx_{H_2O}}{dz} \tag{A3}$$

where

$$x_{H_2O} = \frac{c_{H_2O}}{c}$$

For a binary gas mixture at low pressures, the mass diffusivity $D_{H_2\text{-}H_2O}$ is proportional to a power of temperature, inversely proportional to pressure, and nearly independent of the mixture composition. Since all the water-rejection transients were run at a constant temperature and a constant low pressure, in this analysis the diffusivity can be assumed to be constant. Also, since the mass transfer in the electrode is an equal-molar process, during steady-state operation the molar concentration c of the hydrogen - water-vapor mixture is constant over the thickness of the electrode, and Fick's law becomes

$$N_{H_2O} = -D_{H_2\text{-}H_2O} \frac{dc_{H_2O}}{dz} \tag{A4}$$

where

$$c_{H_2O} = \frac{P_{el}}{M_{H_2O}RT}$$

If the molar flux N_{H_2O} is assumed to be constant over the thickness of the electrode, equation (A4) can be integrated to give

$$N_{H_2O} = \frac{D_{H_2\text{-}H_2O}}{M_{H_2O}RT}\left(\frac{P_e - P_s}{\Delta Z_2}\right) \tag{A5}$$

Therefore, the mass flow of water vapor out of the electrolyte is

$$W_e = 0.89\, N_{H_2O} M_{H_2O} A_z = \frac{0.89\, D_{H_2\text{-}H_2O}(P_e - P_s)A_z}{(\Delta Z_2)RT} \tag{A6}$$

The factor 0.89 represents the ratio of the effective flow area to the geometric area in the direction of flow for an electrode porosity of 80 percent.

Thus, the lumped-parameter equation for the conservation of the mass of water in the electrolyte is

$$\frac{dm_{H_2O}}{dt} = W_r - \frac{0.89\, D_{H_2\text{-}H_2O}(P_e - P_s)A_z}{(\Delta Z_2)RT} \tag{A7}$$

In equation (A7), the partial pressure of the water vapor in the hydrogen stream P_s varies along the stream length. However, since this study is being conducted on a lumped-parameter basis, the average partial pressure in the stream is needed. The steady-state conservation of mass was applied to the hydrogen-gas chamber to determine an expression for a pressure distribution from which this average can be calculated. With the flow along the length of the chamber assumed to be in the x-direction, this equation is

$$\frac{d(\rho_s V_s)}{dx} = \frac{0.89\, M_{H_2O} N_{H_2O}}{\Delta Z_3} \tag{A8}$$

or

$$\frac{1}{A_x}\frac{dW_{H_2O}}{dx} = \frac{0.89\, M_{H_2O} N_{H_2O}}{\Delta Z_3} \tag{A9}$$

The right side of equation (A9) represents the mass flow of water per unit volume entering the gas stream from the hydrogen electrode. Substituting the expression for molar flow (eq. (A5)) into equation (A9) yields

$$\frac{1}{A_x}\frac{dW_{H_2O}}{dx} = \frac{0.89\, D_{H_2\text{-}H_2O}(P_e - P_s)}{(\Delta Z_3)(\Delta Z_2)RT} \tag{A10}$$

An expression relating the stream hydrogen and water-vapor flow rates to their respective partial pressures was used to convert the left side of equation (A10) to a function of the partial pressure of the water vapor in the stream:

$$\frac{P_s}{P_{H_2}} = \frac{\dfrac{W_{H_2O}}{M_{H_2O}}}{\dfrac{W_{H_2}}{M_{H_2}}} = \frac{\dfrac{W_{H_2O}}{18}}{\dfrac{W_{H_2}}{2}}$$

or

$$W_{H_2O} = \frac{9W_{H_2}}{P_{H_2}} P_s$$

Since the total cell pressure was held constant, the change in hydrogen partial pressure P_{H_2} over the length of the cell's gas stream was caused by the flow of water vapor into the stream from the electrode. Because of the small amount of water vapor entering relative to the hydrogen flow rate, this effect on the hydrogen partial pressure was small. Thus, P_{H_2} was assumed to be constant and equal to an average value calculated from the input and output values of the initial steady-state condition. Similarly, the hydrogen flow rate varies over the length of the gas chamber only by the amount of hydrogen that enters into the reaction. This amount too was assumed to be constant and equal to the average of the input and output values. Based on these assumptions, the conservation of mass equation for the gas stream is

$$\frac{9\overline{W}_{H_2}}{A_x\overline{P}_{H_2}} \frac{dP_s}{dx} = \frac{0.89\, D_{H_2\text{-}H_2O}(P_e - P_s)}{(\Delta Z_3)(\Delta Z_2)RT} \tag{A11}$$

The solution of equation (A11) for P_s is

$$P_s = P_e + Ke^{-(m/n)x} \tag{A12}$$

where K is the constant of integration,

$$n = \frac{9\overline{W}_{H_2}}{A_x\overline{P}_{H_2}}$$

and

$$m = \frac{0.89\, D_{H_2\text{-}H_2O}}{(\Delta Z_3)(\Delta Z_2)RT}$$

At $x = 0$, $P_s = P_{s,i}$, and, therefore, the constant of integration is

$$K = P_{s,i} - P_e$$

The equation used to determine the average partial pressure of the stream water vapor over the length L of the gas chamber is

$$\overline{P}_s = \frac{1}{L}\int_0^L \left[P_e + (P_{s,i} - P_e)e^{-(m/n)x}\right]dx \tag{A13}$$

or

$$\overline{P}_s = P_e - \frac{n}{Lm}(P_{s,i} - P_e)e^{-mL/n} + \frac{n}{Lm}(P_{s,i} - P_e) \tag{A14}$$

Thus, substituting this expression for the partial pressure P_s in equation (A7) yields the equation for the conservation of the mass of water in the electrolyte:

$$\frac{dm_{H_2O}}{dt} = W_r - \frac{0.89\, D_{H_2\text{-}H_2O} A_z}{(\Delta Z_2)RT}\left[\frac{n}{Lm}(P_{s,i} - P_e)e^{-mL/n} - \frac{n}{Lm}(P_{s,i} - P_e)\right] \tag{A15}$$

The definition of the concentration of the electrolyte is

$$C = \frac{m_{KOH}}{m_{KOH} + m_{H_2O}}$$

or

$$m_{H_2O} = \frac{1 - C}{C} m_{KOH}$$

where the mass of the potassium hydroxide in the electrolyte m_{KOH} is constant. When substituting this expression for m_{H_2O} in equation (A15), the derivative term becomes

$$\frac{dm_{H_2O}}{dt} = m_{KOH} \frac{d\left(\frac{1}{C}\right)}{dt}$$

Since all the transients were run at constant temperature and pressure, the electrolyte concentration is a function of only the equilibrium partial pressure of water in the electrolyte, and the derivative can be expressed as

$$\frac{dm_{H_2O}}{dt} = m_{KOH} \frac{d\left(\frac{1}{C}\right)}{dP_e} \frac{dP_e}{dt}$$

From vapor-pressure data supplied by the fuel-cell manufacturer, it was found that the relation between the electrolyte concentration and vapor pressure in log coordinates at a given temperature is very nearly linear over a wide range. Since this is the case, an equation for a straight line of the form $C = A - B \log P_e$ can be used to represent the data. The term $d(1/C)/dP_e$ can then be expressed as

$$\frac{d\left(\frac{1}{C}\right)}{dP_e} = \frac{0.434\ B}{P_e C^2}$$

where B represents the absolute value of the slope of the curve of log vapor pressure as a function of concentration. The conservation of mass equation (eq. (A15)) can then be rewritten as

$$\left(\frac{0.434\ B}{P_e C^2}\right)\frac{dP_e}{dt} + \frac{nA_z(\Delta Z_3)(1 - e^{-mL/n})P_e}{Lm_{KOH}} = \frac{W_r}{m_{KOH}} + \frac{nA_z(\Delta Z_3)(1 - e^{-mL/n})P_{s,i}}{Lm_{KOH}} \qquad \text{(A16)}$$

For the fuel cell tested, the equilibrium vapor pressure of the electrolyte P_e can be assumed to be equal to the partial pressure of the water vapor in the hydrogen stream at the fuel-cell outlet $P_{s,o}$. This approximation is based on a calculation which shows that the exponential function of the partial pressure of the water vapor along the length of the gas stream (eq. (A12)) attains 90 percent of its final value within 4 percent of the gas chamber length; the final value is the equilibrium vapor pressure of the electrolyte. Thus, since the electrolyte vapor pressure and the partial pressure of the water vapor in the outlet stream can be assumed to be equal, and since the outlet hydrogen partial pressure can be assumed to be constant, the electrolyte vapor pressure can be expressed as a function of the outlet steam to hydrogen mass ratio. This relation is the parameter recorded by the humidity sensor:

$$P_e = P_{s,o} = \frac{P_{H_2,o}H_o}{9}$$

Similarly,

$$P_{s,i} = \frac{P_{H_2,i} H_i}{9}$$

In addition, it was found by calculation that the term $0.434\ B/C^2 P_e$ could be approximated by a constant over the range covered during any particular transient.

When the preceding approximations are incorporated, the conservation of mass (eq. (A16)) can be written as

$$\frac{dH_o}{dt} + \frac{H_o}{\tau} = \frac{9W_r}{\varphi m_{KOH} P_{H_2,o}} + \frac{P_{H_2,i} H_i}{\tau P_{H_2,o}} \tag{A17}$$

where

$$\varphi = \frac{0.434\ B}{C^2 P_e}$$

and

$$\tau = \frac{L m_{KOH} \varphi}{n A_z (\Delta Z_3)(1 - e^{-mL/n})}$$

APPENDIX B

SYMBOLS

A	constant
A_z	electrode area, $in.^2$; cm^2
A_x	gas-chamber cross-sectional area normal to stream flow, $in.^2$; cm^2
B	slope of log vapor pressure as function of concentration
C	electrolyte concentration, wt fraction
c	total molar concentration of hydrogen - water-vapor mixture, (lb-mole)/$in.^3$; (kg-mole)/cm^3
c_{H_2O}	molar concentration of water vapor in hydrogen - water-vapor mixture, (lb-mole)/$in.^3$; (kg-mole)/cm^3
$D_{H_2\text{-}H_2O}$	mass diffusivity of hydrogen - water-vapor mixture, $in.^2$/sec; cm^2/sec
H_i	fuel-cell stream-inlet steam to hydrogen mass ratio
H_o	fuel-cell stream-outlet steam to hydrogen mass ratio (humidity)
L	hydrogen-gas-chamber length, in.; cm
M_{H_2O}	molecular weight of water vapor, lb mass/(lb mass-mole); kg/(kg-mole)
M_{H_2}	molecular weight of hydrogen, lb mass/(lb mass-mole); kg/(kg-mole)
m_{H_2O}	mass of water contained in electrolyte, lb mass; kg
m_{KOH}	mass of potassium hydroxide contained in electrolyte, lb mass; kg
N_{H_2}	molar flux of hydrogen in electrode, (lb-mole)/($in.^2$-sec); (kg-mole)/(cm^2-sec)
N_{H_2O}	molar flux of water vapor in electrode, (lb-mole)/($in.^2$-sec); (kg-mole)/(cm^2-sec)
P_e	equilibrium vapor pressure of electrolyte, lb/$in.^2$; kg/cm^2
P_{el}	partial pressure of water vapor in electrode, lb/$in.^2$; kg/cm^2
P_{H_2}	partial pressure of hydrogen in gas chamber, lb/$in.^2$; kg/cm^2
$\bar{P}_{H_2}$	average, steady-state, hydrogen partial pressure over length of gas chamber, lb/$in.^2$; kg/cm^2

$P_{H_2,i}$	partial pressure of hydrogen in fuel-cell inlet stream, lb/in.^{2}; kg/cm^2
$P_{H_2,o}$	partial pressure of hydrogen in fuel-cell outlet stream, lb/in.^{2}; kg/cm^2
P_s	partial pressure of water vapor in hydrogen chamber, lb/in.^{2}; kg/cm^2
$P_{s,i}$	partial pressure of water vapor in hydrogen stream at cell inlet, lb/in.^{2}; kg/cm^2
$P_{s,o}$	partial pressure of water vapor in hydrogen stream at cell outlet, lb/in.^{2}; kg/cm^2
R	water-vapor gas constant, (in.-lb)/(lb mass-^oR); (cm-lb)/(kg-^oK)
T	temperature, ^oR; ^oK
t	time, min
V_s	water-vapor flow velocity in gas chamber, in./sec; cm/sec
W_e	water-flow out of electrolyte, lb/sec; kg/sec
$\overline{W}_{H_2}$	hydrogen flow rate in gas chamber, lb/sec; kg/sec
W_{H_2}	average, steady-state, hydrogen flow rate through gas chamber, lb/sec
W_{H_2O}	water-vapor flow rate in gas chamber, lb/sec; kg/sec
W_r	rate of generation of water of reaction, lb/sec; kg/sec
x_{H_2O}	mole fraction of water vapor in hydrogen - water-vapor mixture
ΔZ_2	electrode coarse-pore thickness, in.; cm
ΔZ_3	gas-chamber thickness, in.; cm
ρ_s	vapor density of water vapor in gas chamber, lb/in.^{3}; kg/cm^3
φ	proportionality constant relating electrolyte concentration and electrolyte partial pressure, in.^{2}/lb; cm^2/kg
τ	time constant of lag response of water-rejection model, sec

REFERENCES

1. Prokopius, Paul R.: Use of a Fluidic Oscillator as a Humidity Sensor for a Hydrogen - Steam Mixture. NASA TM X-1269, 1966.

2. Bird, R. Byron; Stewart, Warren E.; and Lightfoot, Edwin N.: Transport Phenomena. John Wiley and Sons, Inc., 1960.

NASA-Langley, 1967 —— 3 E-3763

"The aeronautical and space activities of the United States shall be conducted so as to contribute . . . to the expansion of human knowledge of phenomena in the atmosphere and space. The Administration shall provide for the widest practicable and appropriate dissemination of information concerning its activities and the results thereof."

—NATIONAL AERONAUTICS AND SPACE ACT OF 1958

NASA SCIENTIFIC AND TECHNICAL PUBLICATIONS

TECHNICAL REPORTS: Scientific and technical information considered important, complete, and a lasting contribution to existing knowledge.

TECHNICAL NOTES: Information less broad in scope but nevertheless of importance as a contribution to existing knowledge.

TECHNICAL MEMORANDUMS: Information receiving limited distribution because of preliminary data, security classification, or other reasons.

CONTRACTOR REPORTS: Scientific and technical information generated under a NASA contract or grant and considered an important contribution to existing knowledge.

TECHNICAL TRANSLATIONS: Information published in a foreign language considered to merit NASA distribution in English.

SPECIAL PUBLICATIONS: Information derived from or of value to NASA activities. Publications include conference proceedings, monographs, data compilations, handbooks, sourcebooks, and special bibliographies.

TECHNOLOGY UTILIZATION PUBLICATIONS: Information on technology used by NASA that may be of particular interest in commercial and other non-aerospace applications. Publications include Tech Briefs, Technology Utilization Reports and Notes, and Technology Surveys.

Details on the availability of these publications may be obtained from:

SCIENTIFIC AND TECHNICAL INFORMATION DIVISION

NATIONAL AERONAUTICS AND SPACE ADMINISTRATION

Washington, D.C. 20546